

EREM 81/4Journal of Environmental Research,
Engineering and Management

Vol. 81 / No. 4 / 2025

pp. 79–92

10.5755/j01.erem.81.4.40346

**Application of Activated Carbon from Jojoba Seed Residue
in Refinery Wastewater Treatment**

Received 2025/01

Accepted after revisions 2025/08

<https://doi.org/10.5755/j01.erem.81.4.40346>

Application of Activated Carbon from Jojoba Seed Residue in Refinery Wastewater Treatment

**Shaima Albazzaz^{1*}, Janaen Y. Al-Saeedi², Anwar A. Abbood¹, Harith Y. Mahmood³,
Rusul Naseer Mohammed¹**¹ Department of Chemical Engineering, College of Engineering, University of Basrah, Iraq² Department of Biology, College of Science, University of Basrah, Iraq³ Department of Physiology and Chemistry, College of Veterinary, University of Basrah, Iraq***Corresponding author:** shaima.shueayb@uobasrah.edu.iq

The effluent flowing from oil refineries, which frequently goes into rivers, typically carries a variety of pollutants. In the present study, a quest has been undertaken to investigate the feasibility of using activated carbon prepared from both sub-fermented and unfermented jojoba seed residues for treatment of petroleum refinery wastewater. The biomass were carbonised and thermally activated at 700, 800 and 900°C respectively, then characterized for the adsorption of phenol, chemical oxygen demand (COD), biological oxygen demand (BOD), turbidity, chloride, phosphate, total dissolved solids (TDS), total suspended solid (TSS), pH, electrical conductivity and sulfate ions. The activated carbon obtained from the fermented jojoba residue at 800°C (i.e., SRB2) had, of all samples studied, the highest surface area (959 m²/g) and total pore volume (0.43 cm³/g). The sample showed a good adsorption capacity for not only lowering the COD (chemical oxygen demand reduction 76.29%) and BOD₅ (bio-chemical oxygen demand 75%), but also to reduce turbidity, phenol and inorganic ion.

Although complete phenol removal was not achieved to meet environmental discharge standards, SRB2 showed the best performance among all samples and showed the best fit for Freundlich model isotherm, suggesting multilayer adsorption on a heterogeneous surface. FTIR analysis confirmed the involvement of both physisorption and chemisorption mechanisms, including n–n interactions, hydrogen bonding, and carbonyl-related bonding. SEM and pore size distribution analyses confirmed the micro- and mesoporous structure of SRB2, making it well-suited for phenol adsorption.

These findings highlight the effectiveness of fermented jojoba-derived activated carbon, particularly SRB2, as a sustainable, low-cost bio-adsorbent for reducing organic and inorganic pollutants in petroleum refinery wastewater.

Keywords: petroleum refinery wastewater, jojoba residue, activated carbon, adsorption, isotherms.

Introduction

Petroleum refineries are industries that deal with products with the greatest potential for pollution. These pollutants are generated during the operational processes within refining units or may result from leaks caused by equipment corrosion or failure. The wastewater discharged from these refineries, often into rivers as observed in Iraq, typically contains a variety of organic and inorganic pollutants such as petroleum hydrocarbons, oils, greases, phenol, ammonia, and sulphides. The extremely complex forms of these compounds pose a substantial environmental hazard (Mohammed et al., 2013; Mohammed et al., 2014). Therefore, it is crucial to eliminate the concentration of pollutants to the extent that complies with environmental regulations.

To treat wastewater, a variety of chemical, physical and biological methods have been used including adsorption techniques with activated carbon or metal-organic frameworks (MOFs), membrane separation, photodegradation, aerobic and anaerobic biodegradation, photocatalysis and membrane bioreactor (Joseph et al., 2019) and (Shahabinejad et al., 2024). Activated carbon (AC) is one of the most effective adsorbents for removing pollutants from wastewater even at concentrations as low as parts per million (ppm) (Al-Saeedi et al., 2019; Albazzaz et al., 2024). However, the high cost of activated carbon, especially that obtained from non-renewable resources, represents a major obstacle to the wide spread application of adsorption technology using activated carbon in large-scale or economically limited processes. Additionally, regeneration processes are responsible for the loss of approximately 10–15% of the activated carbon (Remmani et al., 2021; Oghenejoboh et al., 2016). Insights (2020) indicated that the cost of producing one ton of commercial activated carbon is approximately US\$2,000. Consequently, the development of renewable and cost-effective adsorbents is a pressing necessity to further benefit from adsorption technology. In this area, the effectiveness of some available and low-cost agricultural by-products as raw materials for activated carbon such as rice husks, palm oil husks, and coconut shells has been investigated (Kaya et al., 2024; Harimisa et al., 2021; Sher et al., 2020). In Egypt and Jordan, 1990s. Jojoba has begun to be cultivated and then spread to other countries including Iraq. The total area presently cultivated and premeditated in range between 30,000 and

50,000 hectares. Due to the increased domestic cultivation of jojoba and its reasonably low manufacturing costs, jojoba-derivative activated carbon represents a preferred and viable alternative to common commercial products. Allawzi et al. (2010) established that 5 milligrams per milliliter (mg/mL) of jojoba seed residue that remove 9.89 mg/g of cadmium (Cd^{2+}) at 25 ppm of concentration in an aqueous solution. Furthermore, Al-Zoubi et al. (2020) investigated the use of jojoba seed residues to remove anionic dyes from the aqueous phase after the oil extraction and defatting (with n-hexane) techniques. The greater dye removal efficiency is achieved compared to other cultivated by-products, weight the potential of jojoba residue in dye removal from wastewater. In the same way, jojoba seed residues revealed high removal efficiency in removing phenolic compounds at 180°C activated for 2 hours in an electric oven (Abu-Arabi et al., 2007). Other researchers, such as Tawalbeh et al. (2005) performed jojoba seed residue as a raw material to investigate the efficiency of chemically activated carbon with different chemical chemicals: zinc chloride (ZnCl_2), potassium chloride (KCl), and phosphoric acid (H_3PO_4) on iodine removal. The experiments were implemented using a laboratory-scale fixed reactor. The highest iodine adsorption was observed using zinc chloride (ZnCl_2). Phenolic organic mixtures are common in manufacturing wastewater, mostly from petroleum factories. It was necessary to reduce them due to their toxicity to permissible limits remains a challenge for investigators in this field. Activated carbon considered as the most active adsorbents that used to treat phenol, due to its porous configuration. For example, Zhang et al. (2015) achieved phenol adsorption exceeding 60 mg/g from water using rice husk-derived activated carbon after pyrolysis of the raw material. Additionally, the phenol adsorption capacity of wastewater reached 48.58 mg/g using banana peel-derived activated carbon (Ingole et al. (2017)). Despite these promising results, research is still ongoing into alternative raw materials and activation technologies that can enhance the adsorption capacity of activated carbon and meet environmental sustainability standards.

This study aimed to examine the adsorption properties and effectiveness of fermented activated carbon derived from jojoba seed residue in treating refinery wastewater, and to compare its pollutant removal efficiency with that of the raw material and the non-fermented

activated carbon derived from it. Furthermore, the study intended to determine an optimal theoretical heat model that accurately represents the experimental equilibrium data for the most effective sample in adsorption processes. However, this study is distinguished by its emphasis on activated carbon obtained from fermented jojoba residues, as the impact of the fermentation process of the raw materials utilized in the production of activated carbon on adsorption processes has not been previously investigated in depth.

Materials and methods

Materials

Jojoba seeds were obtained from a nursery in Babylon Governorate, Iraq. All chemicals were purchased from Sigma-Aldrich. The wastewater under study (70 liter) was obtained from the Al-Dora refinery in Baghdad, Iraq. This sample was then filtered under vacuum with a Buchner vacuum pump to eliminate any

residual suspended solids and was stored in a securely sealed container at a temperature of 4°C until required. The experiments were conducted in 2024 at the Chemical Engineering Laboratory, University of Basra.

Preparation of activated carbons

In order to prepare the jojoba hulls for activation, a total of 700 grams (g) of hulls were thoroughly cleaned using tap water to eliminate any dust and impurities. Subsequently, the hulls were sun-dried for a period of three days and divided into three distinct groups, 100 g, 300 g, and 300 g, and named SR, SRA, and SRB respectively. Conversely, the SRB group was submerged in an open water container for seven days, with the water being replaced every 24 hours to promote the extraction of cyanogenic glycosides present from the residue. The fermented jojoba residue was rinsed three times with distilled water and then left to dry under direct sunlight for seven days. Finally, SRA, SR, and SRB were crushed individually using a mortar and pestle and filtered using a 500- μ m sieve.

Fig. 1. (a) Jojoba seeds, (b) jojoba seed hulls, (c) ground jojoba seed hulls



In this study, activation of the samples was implemented using method in Tawalbeh et al. (2005) with slight differences. A total of 70 g of the mixture was arranged, consisting of KCl and ZnCl_2 in a 1:1 weight ratio. This combination was separately collective with 6 L of distilled water and 300 g of dried structures from each of SRA and SRB. Secondly, the mixtures were shaken for seven hours at 85°C in a water bath. After that, the mixture was transmitted to the hot zone of a furnace and heating at 105°C for twenty-four hours for evaporation the solution and extract the solid units. The SRA was separated into three sets; SRA1, SRA2 and SRA3, while SRB was separated into SRB1, SRB2 and SRB3 where each group weighing

100 g. Nitrogen gas was passed through each sample in a horizontal tube furnace (Elite Thermal Systems Ltd., UK) for two hours to raise their activation temperatures of both (SRA1, SRB1) to 700°C; (SRA2, SRB2) to 800°C, and (SRA3, SRB3) to 900°C. Then, the samples were detained at these temperatures for an additional hour before reducing the temperature to 250°C to complete the cooling process. Finally, the particles were dried in an oven for 24 hours at 105°C before being stored.

Chemical and physical and characterization of AC

The surface area, pore volume was found out using a Micromeritics Faster Surface Area and Porosimetry

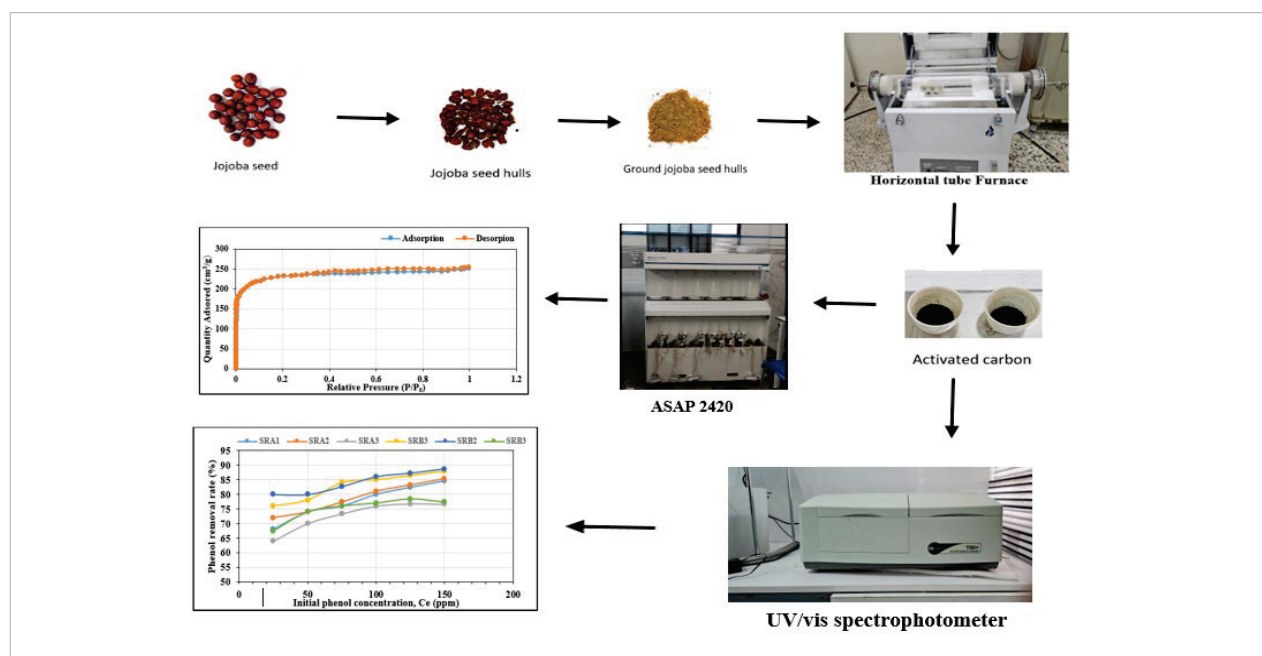
analyzer (Micromeritics Corporation, ASAP 2420). BET equation was used for calculating the surface area of the adsorbents. Fourier transform infrared spectroscopy (FTIR) used before and after adsorption (e.g., phenol adsorption) to study chemical interactions between the adsorbate and the carbon surface

Collection of samples and analysis procedures

A 70-liter wastewater sample was collected in June 2024 from the wastewater treatment plants at the Dora refinery in Baghdad, Iraq. Physicochemical analyses were conducted at the University of Basrah in accordance with standard and recommended procedures (APHA 2005).

The pH and water temperature were measured with a pH meter (SD 300), while turbidity was evaluated using a Lovibond device (TB 300 IR). TDS and EC values were determined using a UBANTE multiparameter water testing device (Model XYZ), with proper calibration conducted prior to measurement. The biological oxygen demand (BOD5) test was conducted in the laboratory with a five-day incubation at 20°C, and the chemical oxygen demand (COD) test was performed using a Lovibond device (RD 125). Total suspended solids (TSS), sulphate (SO_4^{2-}), chloride (Cl^-), and phosphate (PO_4^{3-}) tests were also carried out in the laboratory according to standard methods that illustrated by Beutler et al. (2014).

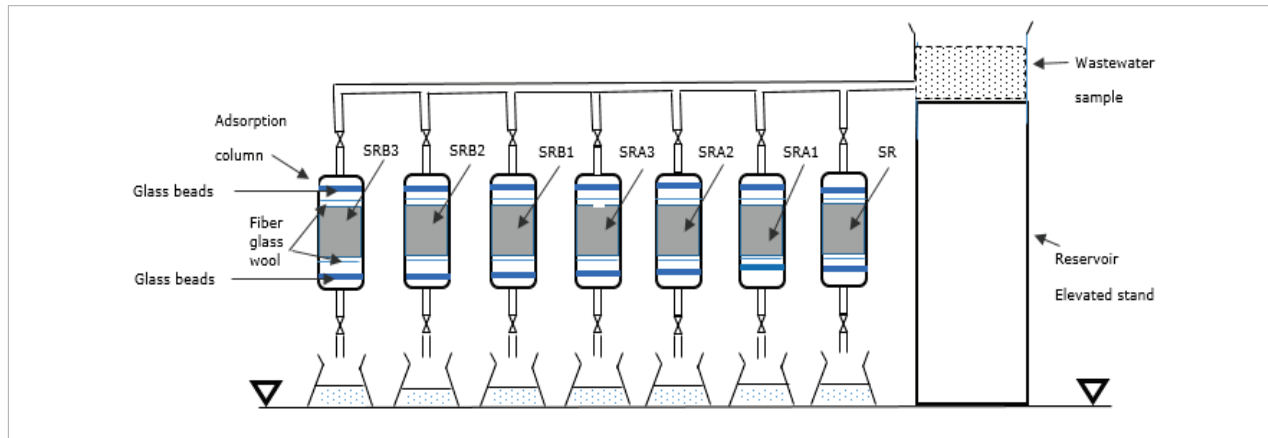
Fig. 2. Graphical abstract



Adsorption test and analysis

Seven equal-sized packed columns (diameter = 4 cm, length = 18.3 cm) were arranged as shown in Fig. 3, each filled with 100 g of one of the samples: SR, SRA1, SRA2, SRA3, SRB1, SRB2, or SRB3. Furthermore, glass beads and wool were placed at the top and bottom of the column. The adsorption process was conducted following the methodology reported by Oghenejoboh et al. (2016), with slight modifications; seven valves were used to connect the container's output to each of the graded seven adsorption columns, allowing the control of the amount of wastewater entering the columns

via gravity. For six hours, the effluents from the seven flasks were collected at 2-hour intervals to conduct triplicate measurements of the adsorption parameters for comparison. All measurements were performed in triplicate, and the standard deviation (SD) for each parameter was within acceptable analytical limits (< 3%), ensuring reproducibility. The COD, BOD5, TDS, pH, conductivity, turbidity, and phenol of the treated effluent and the refinery wastewater were analysed using respective meters, while heavy metal analysis was done using an 82 UV/vis spectrophotometer (Ubi-600, MicroDigital Co., Ltd., Republic of Korea).

Fig. 3. Experimental set-up for fixed-bed activated carbon treatment of refinery wastewater

Results and discussion

The analysis of refinery wastewater before and after treatment

Table 1 presents the analysis of refinery wastewater before and after treatment using raw material and activated carbons derived from both fermented and unfermented jojoba residues. It is clear that the pH values of wastewater treated with activated carbon from fermented jojoba seed residues (SRB1: 6.93, SRB2: 7.21, SRB3: 6.55) were higher than those treated with

activated carbon from unfermented jojoba residues (SRA1: 6.64, SRA2: 6.80, SRA3: 6.43) or treated with raw materials (6.39). The observed transition from acidic to more basic pH in the treated effluent may be attributed to the release of hydrogen ions from the adsorbent surface at the early stages of adsorption. As the process continues, equilibrium is established, and the proton concentration decreases, possibly due to ion exchange, adsorption of acidic compounds, or buffering effects, leading to an increase in pH (Oghenejoboh et al., 2016) and (Kim and An, 2021).

Table 1. Analyses result of refinery wastewater before and after treatment with raw material and activated carbons derived from fermented and unfermented jojoba residues

Parameters	Before treatment	After treatment						
		SR	SRA1	SRB1	SRA2	SRB2	SRA3	SRB3
pH	6.30	6.39	6.64	6.93	6.80	7.21	6.43	6.55
COD (mg/L)	388	279	123	103	111	92	198	183
BOD5 (mg/L)	136	107	48	40	42	34	63	54
Electrical conductivity ($\mu\text{S}/\text{cm}$)	1270	1268	1261	1224	1255	1208	1267	1254
TDS (mg/L)	1180	1173	1054	976	993	947	1125	1107
TSS (mg/L)	215	148	37	25	29	19	58	45
Turbidity (NTU)	92	27.17	69.56	79.34	78.26	85.86	53.26	60.86
PO_4^{3-} (mg/L)	1.24	1.20	1.04	0.94	0.99	0.89	1.16	1.12
Cl^- (mg/L)	1150	1034	627	541	618	523	723	698
Phenol (mg/L)	1.92	1.31	0.51	0.39	0.43	0.42	0.82	0.69
SO_4^{2-} (mg/L)	326	309	268	254	259	241	296	284

COD in wastewater indicates the quantity of oxygen necessary for the chemical oxidation of both organic and inorganic materials present in the water. The concentration of COD in wastewater was reduced by 68.3%, 71.4%, and 49% after treatment with SRA1, SRA2, and SRA3, respectively. In contrast, treatments with SRB1, SRB2, and SRB3 resulted in high reductions of 73.45%, 76.29%, and 52.8%, respectively while the reduction in COD by SR was only 28.01%. While the SRB1 and SRA2 values were close to the allowable limit, the SRB2 sample, which showed 92 mg/L, was lower than the allowable limit for COD set by Iraqi standards and the United States Environmental Protection Agency (EPA) specifications, which is 100 mg/L (Abdulkareem et al., 2021) and (EPA, 2007). In fact, at higher pH levels, the solubility of specific organic compounds reduces, causing them to hurried or adsorb onto solid particles. This phenomenon releases them for oxidation and therefore the measured COD decreases. After they adsorption by the SR, pH of the wastewater increased due to hydrolysis reactions that led the organic substances in wastewater releasing hydroxide ions (OH^-). This increase reduces the oxidation sensitivity of the materials and influences in this way COD of liquid waste. Moreover, the wastewater pH was increased after adsorption process using activated carbon derived from unfermented and fermented jojoba seed; having SRB1 and SRB2 reached highest alkaline condition. This suggests that the surface properties of the carbon are altered after fermentation and hence its efficiency in removing acidic compounds from wastewater is increased. The degradation of COD content in wastewater was further proved to be better when using fermented carbonized sawdust, indicating that fermented activated carbon played a role in the degradation of organic pollutants.

The pH and COD values of samples SRA3 and SRB were lower than those for the activated carbon sample prepared at lower temperature. It indicates that the 900°C prepared activated carbon may have less activity of functional groups or damage to the pore structure. On the other hand, BOD_5 is an important environmental factor that determines how much biodegradable organic materials are present in wastewater and reflects the amount of oxygen absorbed by microbes over a five-day period (Maddah, 2022). The BOD_5 value of Wastewater after SRA1, SRA2 and SRA3 treatments was reduced by 64.71%, 69.12% and 53.68% respectively with

higher reductions for SRB1(+70.59%), SRB2 (+75%) and SRB3 (60.29%). Only a 21.32% reduction in BOD_5 occurred post-SR treatment. The activated carbon in reduction of BOD_5 of wastewater has a very good efficiency but only for its particle surface area. The larger specific surface area is propitious for adsorbing organic pollutants, promoting microbial growth, and further obviously realizing the COD removal. The organic substances were effectively removed from the effluent by activated carbon to a great extent, which decreased BOD_5 of wastewater too low level (Shah et al., 2023). In addition, the pore size distribution of activated carbon also influences BOD_5 in wastewater. Micropores can only capture small organic molecules, where large organic compounds are primarily adsorbed by mesopores and macropores (Yan et al., 2015). All samples exceeded the permissible limits according to Iraqi standards and EPA, but sample (SRB2), with a value of 34 mg/L, was the nearest to the allowed limit for this element that equals 20 mg/L.

The electrical conductance, a measure of the ability of discharged water to carry electric current, generally depends on concentrations and mobilities (the average particle speed) of ions in water. Water conductance generally increases with higher TDS concentration, due to the fact that more ions in water enhance conductivity. Nevertheless, TDS and EC did not significantly change after treatment in this study. These findings are consistent with those of Ilaboya et al. (2013) observed a low TDS removal associated with adsorption in wastewater. The Total Suspended Solids (TSS) concentration, however, was affected and significantly altered after the treatment. This difference is an indication that solid matters like sand, silt, clay particles, oil droplets, grease and other organic materials derived from petroleum refinery processes found in the wastewater were markedly influenced by use of activated carbon prepared from fermented or unfermented feedstock unlike what was obtained with raw material. However, only the SRB2 sample was lower than the allowable limit set by Iraqi standards and EPA specifications, which is 25 mg/l (Abdulkareem et al., 2021). The fermentation process reduced the cyanide concentration in the raw material and increased the pH values, which were further elevated during the activation process at 700°C and 800°C. Consequently, activated carbons from fermented jojoba residues are particularly effective for the adsorption of organic and trace

pollutants from wastewater (Alinnor and Nwachukwu, 2012). For phenol, the fermented adsorbents showed slightly better performance with increasing pH values of the wastewater, achieving a removal range of 64.06% to 78.12% compared to the 57.29% to 77.60% range observed with unfermented adsorbents, while the reduction of phenol by SR was only 31.77%. EPA has set forth regulations requiring that the phenol content in wastewater be reduced to under 1 mg/L (EPA, 2007). None of the samples in this study succeeded in reducing the phenol concentration to the industry-permissible limit. The findings revealed that the fermentation process of activated carbon does not improve the adsorption of phenol from wastewater, as there was no notable difference between the results of the fermented and non-fermented samples and the pH value of the solution plays an important role in increasing the adsorption of phenol with constant surface area. The results of this study agree with the observations noted by Oghenejoboh et al. (2016) and Allawzi et al. (2010), which indicate that the ability of the adsorbent to remove organic compounds from wastewater increases with an increase in the pH value of the solution. Negative ions (e.g., Cl^- and PO_4^{3-}) adsorption, on the other hand, depends on pH. Under an acidic condition, the abundant H^+ ions may induce that the surface functional groups of adsorbents are ionized and thus become positively charged on the surfaces. This phenomenon causes an increase of the electrostatic attraction between adsorbents and the negatively charged ions as well (Foo and Hameed, 2010). On the contrary, with an increase in pH (H^+ ion concentration decreases), new adsorption sites for these ions are generated at the surface of the adsorbent. This phenomenon could be attributed to the lower amounts of Cl^- and PO_4^{3-} ions given out by fermented adsorbents SRB1 and SRB2 (Shi et al., 2011; Cruz-Lopes et al., 2021).

The nature of the adsorbent surface changes (increased porosity, generation or modification of functional groups) during fermentation. This increase could result in more available and accessible adsorption sites, making these fermenting samples to be beneficial as opposed to other activated AAs especially for higher pH values (alkaline) (Shi et al., 2011; Cruz-Lopez et al., 2011). In addition, the existence of Cl^- ions can effectively suppress the adsorption capacity of phenol because of the intense competition between them for the same active sites. The influence of phosphate ions

on phenol degradation was also observed, although it was not as intensive as that of NO_3^- + 4-OHPs. Bound water film was competed by phenol as well as coexisting ions, as for all samples containing the ions were unable to completely remove the phenol.

The importance of adsorption in capturing suspended solids and dissolved organics for a significant decrease in turbidity provided by activated carbon was already pointed out in section 3. Turbidity of processed waste water applying SRB2 and SRA2 was decreased by 78.26% and 85.86%, respectively. The rest reduced by modest amounts. However, the turbidity values are still above the environmental discharge standards for turbidity in wastewater in Iraq, which is established at 5 NTU (Nephelometric Turbidity Units) (Ghawry and Ghazi, 2017). In addition, no significant change in the concentration of sulfate ions was recorded after adsorption processes for all samples.

It is important to mention that no clogging was observed in the packed column during the six-hour adsorption test using powdered activated carbon (PAC). The system maintained stable flow conditions throughout the experiment.

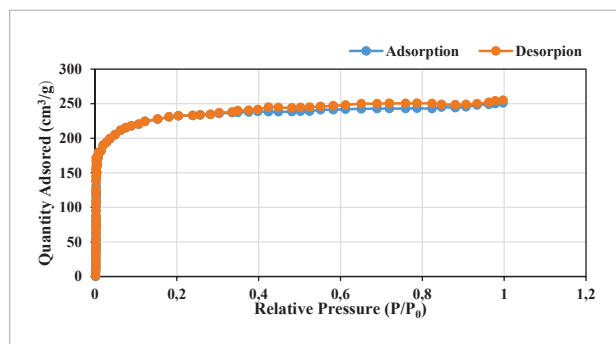
Surface area and porosity of ACS

Table 2 summarizes the textural properties of jojoba residue, as well as fermented and unfermented activated carbons. Typically, the specific surface area and total pore volume of fermented activated carbon are the highest. Fermentation processes often create additional micropores or enhance existing ones, increasing the surface area and pore volume of activated carbon (Cheng et al., 2024). This, with increasing temperature to 800°C, improves its adsorption capacity, this could be due to the fact that most of the non-carbon elements were eliminated during the heating process making it more effective for various applications compared to unmodified activated carbon. According to Tables 1 and 2, SRB2 has the highest surface area, pore volume, and removal capacity, proving it to be the most effective sample for removing pollutants from wastewater compared to the others. Therefore, further experiments will be conducted on this sample. It is important to mention that the elevation of temperature to 900°C may induces a collapse in the structural framework in SRA3 and SRB3 samples, which subsequently leads to a reduction in both surface area and pore volume.

Table 2. Specific surface area and total pore volume of samples

Samples	SR	SRA1	SRB1	SRA2	SRB2	SRA3	SRB3
Specific surface area m ² /g	528	831	886	860	959	714	731
Total pore volume cm ³ /g	0.3	0.36	0.39	0.39	0.43	0.27	0.28

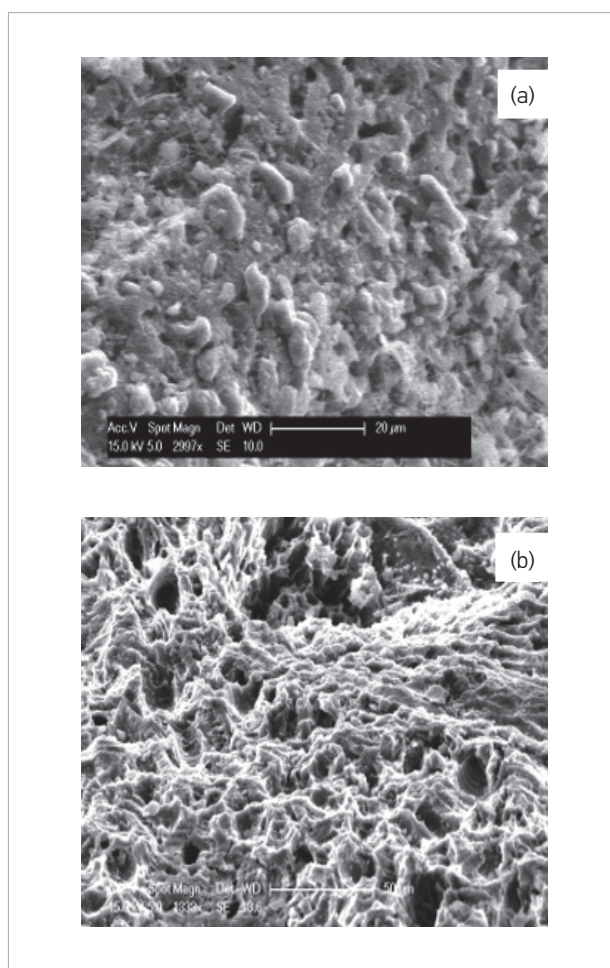
Fig. 4 N₂ adsorption isotherms at 77 K of SRB2 are shown in Fig. The shape of the curve is a signature of type IV isotherm according to IUPAC and comparable with mesoporous materials like AC. The first pattern is observed due to the fill up of the micropores, which is similar to Type I ISO pattern that can be attributed to rapid uptake arising from high affinity with small pores. The isotherms show a significant upward turn at high relative pressures, revealing that the mesopores experience capillary condensation. This point of inflection indicates the hierarchical porous nature that exists in the material and process involving micropores and mesopores contribute to its adsorption capacity. Type I and Type IV isotherm are widely observed for activated carbons, which have a complicated texture usually containing a microporous skeleton having accessible mesoporous surfaces (Albazzaz, 2020).

Fig. 4. Nitrogen adsorption isotherms at 77 K of SRB2

Scanning electron microscopy of activated carbons

The morphologies of the examined activated carbons (SR and SRB2) were examined using a Quanta 600 scanning electron microscope (SEM) in μm scale (Fig. 5). The SR sample reveals a surface structure characterized by rough and heterogeneous pores of varying sizes. Conversely, the SRB2 sample shows a highly porous structure with irregularly shaped and aggregated particles indicating the effectiveness of the activation process in

developing pore structures on the precursor's surface. In addition, crevices are apparent on the porous surface, creating a heterogeneous appearance with a wide range of randomly distributed mesopores of different sizes.

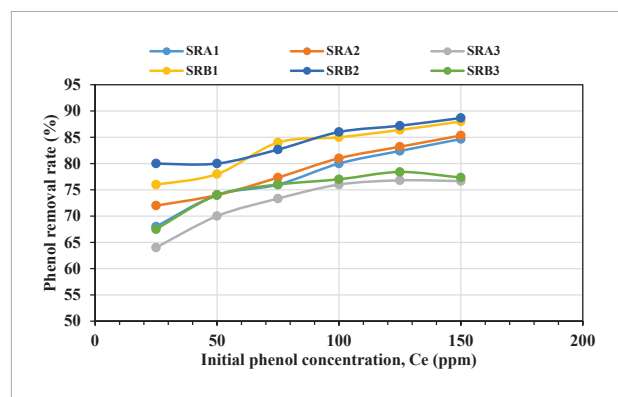
Fig. 5. SR(a) and SRB2(b) Morphology: Effect of initial phenol concentration on removal efficiency with fermented/unfermented adsorbate

The adsorbed phenol removal on SRA1, SRA2, SRA3, SRB1, SRB2 and SRB3 is illustrated in Fig. 6. In the beginning of concentration (a large concentration rise) adsorption efficiency (R%) for activated carbon rose

slowly and then decreased at further rise of phenol concentration. This general trend can be explained due to that the active sites on the adsorbent's surface are-available for reaction occupied by phenol ions presented in solution (Li et al., 2019). The phenol ions may exceed the number of active sites when the phenol concentration is high. It was found that especially for high initial phenol concentrations (C_e) the enhancement of phenol removal efficiency was significant.

For example, the SRA1 removal rate was 68% at 25 ppm and increased to higher than 84% at 150 ppm. Likewise, SRB2 showed a removal capacity of 80% at 25 ppm and then up to 89% at 150 ppm. SRA2 and SRB1 exhibited moderate removal rates in the ranges described above. This trend can be attributed to the higher C_e concentration of phenol, which would indulge a stronger interaction with AC and also it could provide sufficient driving force necessary for surpassing the mass transfer resistance between adsorbent and adsorbate (Srivastava et al., 2006).

Fig. 6. The effectiveness of the removal of phenol as a function of different doses for initial concentration of phenol



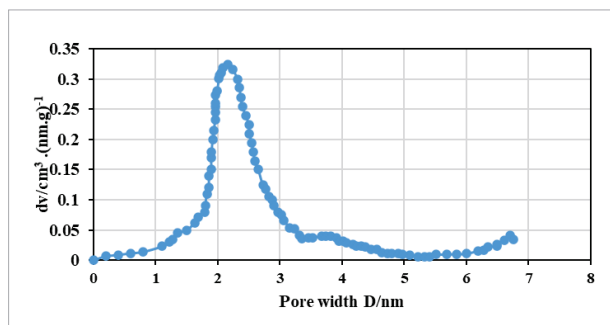
On the contrary, lower adsorption of phenol on SRB3 and SRA3 is observed with respect to other samples (as shown in figure). Moreover, in the other samples (i.e., iPad, and host (100 and 150 ppm)), at higher concentrations an equilibrium was reached with respect to the adsorbent confirming that their pore volume has been filled with phenol molecules. It can be inferred that such fermented adsorbents showed better efficiency for adsorption than non-fermented materials as a whole. Adsorption capacities were similar for all dosages considered, but sample SRB2 proved to be the

most efficient and with a higher capacity for phenol removal from solution.

Pore size distribution

It is awkward to discuss a micropore size distribution with only a single isotherm, so an accurate analysis of this distribution should be made. Usually, the uptake of adsorbate molecules on to the surface of adsorbents is determined by their average pore sizes. The pore size is very important for adsorption to occur and the diameter should be larger than that of adsorbate molecules. As shown in Fig. 7, the pore size of SRB2 has ranging from 1 to 4 nm, which means that there are two types of porosity: microporose (< 2nm) and mesoporose (2–50 nm). The molecular diameter of phenol was 0.75 nm (Lorenc-Grabowska, 2016; Xie et al., 2020). It can be seen that the SRB2 surface is very active for phenol molecule adsorption. Combination of these two types of pores has a higher adsorption nature to the adsorbate molecules.

Fig. 7. Distribution of pore size

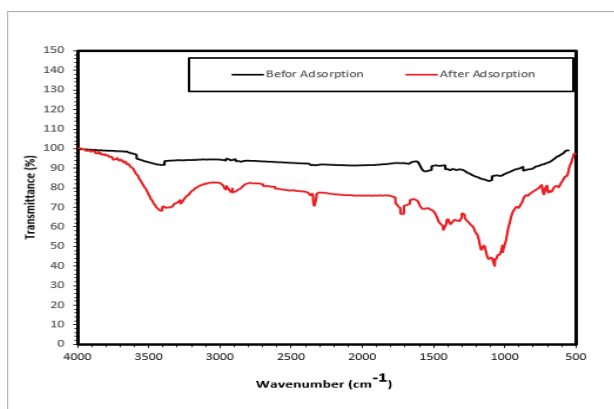


FTIR investigation

The FTIR spectrum of SRB2 prior to adsorption displayed a broad band at 3431.2 cm^{-1} , attributed to O–H stretching vibrations of hydroxyl groups. A distinct absorption was also observed at 1561.2 cm^{-1} , which can be assigned either to C=C stretching in aromatic structures or to asymmetric stretching of carboxylate (COO^-) groups (Socrates, 2004; Coates, 2000). The strength of the oxygen-hydrogen band decreased meaningful after phenol adsorption. That led to the participation of OH-groups in hydrogen connection with phenol molecules. Fig. (8) shows the band was 1561.2 cm^{-1} and budged to approximately 1504 cm^{-1} , which is reliable with n–n interactions between the aromatic ring of phenol

and the carbon surface. Additionally, at 1045.9 cm^{-1} , a new absorption band seemed corresponding to carbon and oxygen band extending vibrations in phenolic constructions. It was noticed that at 2681.8 and 2761.1 cm^{-1} , weak features were appeared. There is a band at 3301.4 cm^{-1} give a further supports the envelopment of H-H bonding interactions (Dąbrowski, 2001). Furthermore, an obvious peak was noticed in 1700 cm^{-1} , corresponding of carbon and oxygen band vibrations. This may indicate the presence of ketone groups on the activated carbon surface, possibly generated or exposed through mild oxidative interactions with phenol (Bansal and Goyal, 2005). Taken together, these spectral changes including band disappearance, shifts in position, and the emergence of new features suggest that phenol adsorption onto SRB2 occurs through a combination of physisorption (via π - π interactions) and chemisorption (through hydrogen bonding and carbonyl-related interactions). Minor oxidative modifications also appear to contribute to the overall adsorption process (Foo and Hameed, 2012).

Fig. 8. FTIR analysis for jojoba residue created activated carbon for both before adsorption (A) and after adsorption (B)



Adsorption isotherms model

The experimental equilibrium was fitted using two adsorption models, Freundlich and Langmuir to identify which model give the best fit for the equilibrium adsorption of phenol from aqueous solutions on SRB2. Langmuir model is based on the assumptions that the surfaces are energetically homogeneous, each active site adsorbs only one molecule, the activity of the active site is not affected by neighbouring sites, the adsorbed

molecules do not interact with each other, and the adsorption is in only one layer; monolayer adsorption, using Eq. 1 (Sahu and Singh, 2019):

$$\frac{C_e}{q_e} = \frac{1}{Q_m K_L} + \frac{1}{Q_m} C_e \quad (1)$$

where C_e the concentration of adsorbate (mg/L); q_e is the amount of solute adsorbed at equilibrium (mg/g); Q_m is the maximum adsorption capacity (mg/g); K_L is the sorption constant (L/mg) at a given temperature.

The Freundlich model is an empirical equation that explains adsorption as a phenomenon occurring across a heterogeneous surface, characterized by a heterogeneity factor of $1/n$. It assumes that adsorption occurs in multiple layers, using Eq. 2 (Salim et al., 2021):

$$\ln q_e = \ln K_f + \frac{1}{n} \ln C_e \quad (2)$$

where K_f is the first Freundlich constant, which represents the adsorption capacity, and n is the second Freundlich constant, which represents the adsorption intensity. Both constants depend on the temperature and the nature of the absorbing surface. Fig. 9 shows each isotherm along with the models that demonstrated good fitting to the data. The constants for the models are given in Table 3. Despite the similar values of the high correlation coefficient (R^2) in the two models, the Freundlich model demonstrates superior correlations with the sample investigated. Significantly, adsorption tends to be more advantageous when the adsorbent has a Freundlich exponent (n) that is greater than 1.

Fig. 9. Adsorption isotherm models (Langmuir and Freundlich) fit for the equilibrium sorption data of phenol from aqueous solutions on SRB2

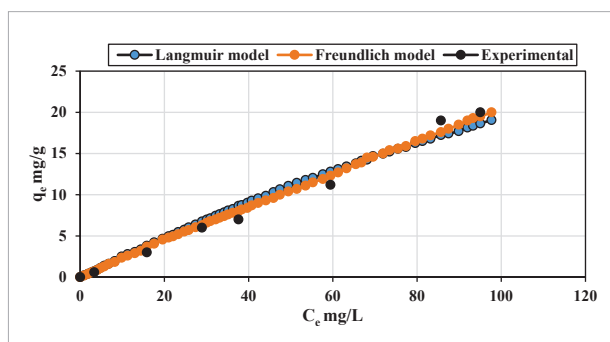


Table 3. Adsorption isotherm parameters and correlation coefficients calculated for Langmuir and Freundlich models at 25°C for phenol on SRB2

Adsorption isotherm model	Langmuir		Freundlich			
	Q_m	K_L	R^2	K_f	n	R^2
Activated carbon						
SRB2	83.7	0.0053	0.981	0.341	1.132	0.991

Conclusions

Petroleum refinery effluents (PRE) represent a major source of pollution within the natural ecosystem. These pollutants are characterized by their rapid spread on the surface of the water, where they form a thin layer on the surface of the water that prevents the exchange of gases with the atmosphere. The results of this study established that activated carbon produced from fermented and unfermented agricultural waste, such as jojoba nut residue (designated as SRA1, SRA2, SRB1, and SRB2, and synthesized through thermal treatment at 700 and 800°C), holds promise for the treatment of wastewater containing organic materials like phenol and trace inorganic pollutants such as Cl^- and PO_4^{3-} ions. The adsorption capacity of the samples activated at 900°C decreased significantly and this was accompanied by a decrease in the surface area porosity. Increased surface area of activated carbon is important since its effectiveness depends on molecular interaction, which can be improved with a larger surface. The result of this study confirms that SRB2 has a greater adsorption capacity than the other samples, and can be used as an efficient candidate for water treatment systems for pollutant removal based on large reduction rates in headwater organic parameters including turbidity, BOD5 and COD. Two isotherm models (Langmuir and Freundlich) have been applied to the adsorption of phenol on SRB2 but obtained data are better fitted by the Freundlich equation that a good agreement between P/F value and R^2 higher than 0.99 was observed here.

The predicted adsorption of SRB2 from the Langmuir model (83.7 mg/g) is not based on an optimal fit, but provides a convenient reference point and indicates that SRB2 has a relatively high adsorption capacity as reported previously for other activated carbons.

Higher adsorption performance of SRB2 could be concluded to its more active sites by a biosorbent or specific surface area, indicating that SRB2 has the potential as phenol-biosorbents. It compares well not only with the above mentioned materials, but also suggest that it's particular functional configuration and microporous character (originating from Thermal/Acid treated Fermented activated carbon) may be responsible for its excellent capacity towards organic pollutant uptake from aqueous medium. Besides, the adsorption peaks in FTIR spectra of hydroxyl and carboxyl groups may exert some effect on the phenol adsorption process. The narrow standard deviation in the phenol adsorption capacity (± 2.1 mg/g) suggests that the surface chemistry is consistent and that the coating method provided a well-reproducible nanomaterial.

Phenol molecules can complexed with COOH group by ionic and non-ionic form to higher adsorptions. In addition, the hydrogen-bonding interactions between phenol and hydroxyl groups are likely to contribute to phenol adsorption through the formation of H-bonds. These results suggest that the adsorption of phenolics on activated carbon is greatly influenced by chemical properties of its surface. Compared with GAC, [that] of phenol is controlled by π - π interaction with the carbon and it is less influenced from alkane groups. The competitive adsorption between phenol and accompanying ions such as Cl^- and PO_4^{3-} was responsible for the decrease in the removal ratio of phenol because there were excessive chloride ions competing with surface adsorption sites. The Cl^- /phenol removal in resin solution/ns-BAC fit the monolayer model with high R^2 values. The results of the studies show high Cl^- uptake and incomplete phenol adsorption, implying that competition prevents phenol from reaching active sites. Phosphate anions hinder the phenol removal as well, even not competitive one.

This study indicates that SRB2 is a promising adsorbent for pollutant removal. With its distinct structural characteristics such as high specific surface area and micro- and meso-porosity, it is considered to be a superior adsorbent for many pollutants.

Powdered activated carbon (PAC) is known to clog easily in packed columns due to its fine particle size, and establishing running conditions also did not show such problems for the present. This behaviour could be due to the small time period over which the experiment

was carried out, the presence of glass beads and wool material both above and below the supporting layers of columns, as well as low flow rates used. Together, these lead to an even flow distribution, that reduced particle sliding, i.e., agglomeration and thus guaranteed hydraulic stability. This study also demonstrates that the abundant jojoba seed byproduct can be a useful source for obtaining cost-effective sorbent to be employed for pollutant removal from refinery wastewater.

References

- Abdulkareem F.A., Hussain T.A., Najaf A.A.N. (2021) The treatment of wastewater produced from Al-Doura refinery to increase production and minimize pollutant Materials. *Iraqi Journal of Science* 62(11): 3984-3996. Available at: <https://doi.org/10.24996/ijis.2021.62.11.19>
- Abu-Arabi M.K., Allawzi M.A., Al-Zoubi A.S. (2007) Adsorption of phenol from aqueous solutions on jojoba nuts residue. *Chemical Engineering & Technology* 30(4): 493-500. Available at: <https://doi.org/10.1002/ceat.200600378>
- Albazzaz S., Al-Saeedi J.Y., Abbood A.A., Mahmood H.Y., Mohammed R.N. (2024) The removal of azo dyes from an aqueous solution using NaOH-activated carbon from phenolic resin. *Environmental Research, Engineering and Management* 80(4): 92-100. Available at: <https://doi.org/10.5755/j01.erem.80.4.37236>
- Albazzaz S. (2020) Understanding and minimising water vapour co-adsorption for activated carbons in post-combustion CO₂ capture. Doctoral dissertation, The University of Nottingham, United Kingdom.
- Alinnor I.J. and Nwachukwu M.A. (2012) Removal of phenol from aqueous solution onto modified fly ash. *International Journal of Research in Chemistry and Environment* 2(2): 124-129. Available at: <https://www.researchgate.net/publication/311584012>
- Allawzi M., Al-Asheh S., Allaboun H., Borini O. (2010) Assessment of the natural jojoba residues as adsorbent for removal of cadmium from aqueous solutions. *Desalination and Water Treatment* 21(1-3): 60-65. Available at: <https://doi.org/10.5004/dwt.2010.1192>
- Al-Saeedi J.Y., Akbar M.M., Al-Qarooni I.H. (2019) Removal of Pb (II) and Ni (II) ions from aqueous solution by sea snail shells. *Journal of Biodiversity and Environmental Sciences* 14(3): 17-23. Available at: <https://www.researchgate.net/publication/332037317>
- Al-Zoubi H., Zubair M., Manzar M.S., Manda A.A., Blaisi N.I., Qureshi A., Matani A. (2020) Comparative adsorption of anionic dyes (eriochrome black T and Congo red) onto jojoba residues: isotherm, kinetics and thermodynamic studies. *Arabian Journal for Science and Engineering* 45: 7275-7287. Available at: <https://doi.org/10.1007/s13369-020-04418-5>
- APHA (American Public Health Association) (2005) Standard Methods for the Examination of Water and Wastewater. 21st edn. Washington, DC: American Public Health Association. ISBN: 978-0875530475
- Bansal R.C. and Goyal M. (2005) Activated Carbon Adsorption. Boca Raton: CRC Press. ISBN: 978-0824753443. Available at: <https://doi.org/10.1201/9781420028812>
- Beutler M., Wiltshire K.H., Meyer B., Moldaenke C., Lüring C., Meyerhöfer M., Hansen U.P. (2014) Monitoring of water quality using fluorescence technique: prospect of on-line process control. *Dissolved Oxygen Dynamics: Case Study of a Subtropical Shallow Lake* 217: 95.
- Cheng S., Cheng X., Tahir M.H., Wang Z., Zhang J. (2024) Synthesis of rice husk activated carbon by fermentation osmotic activation method for hydrogen storage at room temperature. *International Journal of Hydrogen Energy* 62: 443-450. Available at: <https://doi.org/10.1016/j.ijhydene.2024.03.092>
- Coates J. (2000) Interpretation of infrared spectra: a practical approach. *Encyclopedia of Analytical Chemistry* 12: 10815-10837. Available at: <https://doi.org/10.1002/9780470027318.a5606>
- Cruz-Lopes L.P., Macena M., Esteves B., Guiné R.P. (2021) Ideal pH for the adsorption of metal ions Cr⁶⁺, Ni²⁺, Pb²⁺ in aqueous solution with different adsorbent materials. *Open Agriculture* 6(1): 115-123. Available at: <https://doi.org/10.1515/opag-2021-0225>
- Dąbrowski A. (2001) Adsorption –from theory to practice. *Advances in Colloid and Interface Science* 93(1-3): 135-224. Available at: [https://doi.org/10.1016/S0001-8686\(00\)00082-8](https://doi.org/10.1016/S0001-8686(00)00082-8)
- EPA (Environmental Protection Agency) (2007) The Water Sourcebook. Grade level 9-12 Fact sheets. United States Environmental Protection Agency (EPA). Available at: <https://nepis.epa.gov/Exe/ZyPURL.cgi?Dockey=P100IGR8.TXT>
- Foo K.Y. and Hameed B.H. (2010) Insights into the modeling of adsorption isotherm systems. *Chemical Engineering Journal* 156(1): 2-10. Available at: <https://doi.org/10.1016/j.cej.2009.09.013>

Investigations are needed to develop the applications of these adsorbents and solve the operational problems in the pilot stage.

Acknowledgement

The authors would like to gratitude the Lab staff of the Department of Chemical Engineering, University of Basra, Iraq for their technical support throughout this work.

- Foo K.Y. and Hameed B.H. (2012) Potential of activated carbon adsorption processes for the remediation of nuclear effluents: a recent literature. *Desalination and Water Treatment* 41(1–3): 72–78. Available at: <https://doi.org/10.1080/19443994.2012.664698>
- Ghawry A.H. and Ghaziy J.K. (2017) Iraqi water treatment plants process control by measuring effluent turbidity. *Al-Qadisiyah Journal for Engineering Sciences* 3(4): 373–381. Available at: <https://www.iraqoj.net/iasj/download/4e97a4845f7eb9ce>
- Harimisa G.E., Jusoh N.W.C., Tan L.S., Ghafar N.A., Masudi A. (2021) Adsorption of Contaminants from Palm Oil Mill Effluent Using Agricultural Biomass Wastes as Adsorbents. *IOP Conference Series: Materials Science and Engineering* 1051(1): 012062. Available at: <https://doi.org/10.1088/1757-899X/1051/1/012062>
- Ilaboya I.R., Oti E.O., Ekoh G.O. and Umukoro L.O. (2013) Performance of activated carbon from cassava peels for the treatment of effluent wastewater. *Iranica Journal of Energy & Environment* 4(4). Available at: <https://doi.org/10.5829/idosi.ijee.2013.04.04.08>
- Ingle R.S., Lataye D.H. and Dhorabe P.T. (2017) Adsorption of phenol onto banana peels activated carbon. *KSCE Journal of Civil Engineering* 21(1):100–110. Available at: <https://doi.org/10.1007/s12205-016-0101-9>
- Insights F.B. (2020) Activated carbon market size, share & COVID-19 impact analysis, by type (powdered, granular, and others), by application (water treatment, air & gas purification, food & beverage, pharmaceutical & healthcare treatment, and others), and regional forecast, 2022–2030. Report ID: FBI102175. Available at: <https://www.fortunebusinessinsights.com/activated-carbon-market-102175>
- Joseph L., Jun B.M., Jang M., Park C.M., Muñoz-Senmache J.C., Hernández-Maldonado A.J., Heyden A., Yu M. and Yoon Y. (2019) Removal of contaminants of emerging concern by metal-organic framework nano-adsorbents: A review. *Chemical Engineering Journal* 369: 928–946. Available at: <https://doi.org/10.1016/j.cej.2019.03.173>
- Kaya N., Carus Özkese E. and Yıldız Uzun Z. (2024) Investigating the effectiveness of rice husk-derived low-cost activated carbon in removing environmental pollutants: a study of its characterization. *International Journal of Phytoremediation* 26(3): 427–447. Available at: <https://doi.org/10.1080/15226514.2023.2246584>
- Kim T. and An B. (2021) Effect of hydrogen ion presence in adsorbent and solution to enhance phosphate adsorption. *Applied Sciences* 11(6): 2777. Available at: <https://doi.org/10.3390/app11062777>
- Li Y., Wang H., Zhao W., Wang X., Shi Y., Fan H., Sun H. and Tan L. (2019) Facile synthesis of a triptycene-based porous organic polymer with a high efficiency and recyclable adsorption for organic dyes. *Journal of Applied Polymer Science* 136(39):47987. Available at: <https://doi.org/10.1002/app.47987>
- Lorenc-Grabowska E. (2016) Effect of micropore size distribution on phenol adsorption on steam activated carbons. *Adsorption* 22: 599–607. Available at: <https://doi.org/10.1007/s10450-015-9737-x>
- Maddah H.A. (2022) Predicting optimum dilution factors for BOD sampling and desired dissolved oxygen for controlling organic contamination in various wastewaters. *International Journal of Chemical Engineering* 2022(1): 8637064. Available at: <https://doi.org/10.1155/2022/8637064>
- Mohammed R.N., Abualhail S. and Lv X. (2013) Fluidization of fine particles and its optimal operation condition in multimedia water filter. *Desalination and Water Treatment* 51(22–24): 4768–4778. Available at: <https://doi.org/10.1080/19443994.2013.769490>
- Mohammed R.N., Abu-Alhail S. and Wu L.X. (2014) Inter-cross real-time control strategy in a novel phased isolation tank step feed process for treating low C/N real wastewater under ambient temperature. *Korean Journal of Chemical Engineering* 30(10): 1798–1809. Available at: <https://doi.org/10.1007/s11814-014-0107-2>
- Oghenejoboh K.M., Otuagoma S.O. and Ohimor E.O. (2016) Application of cassava peels activated carbon in the treatment of oil refinery wastewater – a comparative analysis. *Journal of Ecological Engineering* 17(2). Available at: <https://doi.org/10.12911/22998993/62290>
- Remmani R., Makhloufi R., Miladi M., Ouakouak A., Canales A.R. and Núñez-Gómez D. (2021) Development of low-cost activated carbon towards an eco-efficient removal of organic pollutants from oily wastewater. *Polish Journal of Environmental Studies* 30(2): 1801–1808. Available at: <https://doi.org/10.15244/pjoes/125765>
- Sahu O. and Singh N. (2019) Significance of bioadsorption process on textile industry wastewater. In: *The Impact and Prospects of Green Chemistry for Textile Technology*. Woodhead Publishing 367–416. Available at: <https://doi.org/10.1016/B978-0-08-102491-1.00013-7>
- Salim N.A.A., Puteh M.H., Khamidun M.H., Fulazzaky M.A., Abdullah N.H., Yusoff A.R.M., Zaini M.A.A., Ahmad N., Lazim Z.M. and Nuid M. (2021) Interpretation of isotherm models for adsorption of ammonium onto granular activated carbon. *Biointerface Research in Applied Chemistry* 11(2): 9227–9241. Available at: <https://doi.org/10.1016/B978-0-08-102491-1.00013-7>
- Shah H.H., Amin M., Pepe F., Mancusi E. and Fareed A.G. (2023) Overview of adsorptive water treatment applications. *Environmental Science and Pollution Research* 32:19084–19108. Available at: <https://doi.org/10.1007/s11356-023-30540-6>
- Shahabinejad H., Binazadeh M., Esmaeilzadeh F., Hashemi F. and Mousavi S.M. (2024) Optimization of cerium-based metal–organic framework synthesis for maximal sonophotocatalytic tetracycline degradation. *Scientific Reports* 14(1): 16887. Available at: <https://doi.org/10.1038/s41598-024-67676-5>

- Sher F., Iqbal S.Z., Albazzaz S., Ali U., Mortari D.A. and Rashid T. (2020) Development of biomass-derived highly porous fast adsorbents for post-combustion CO₂ capture. *Fuel* 282: 118506. Available at: <https://doi.org/10.1016/j.fuel.2020.118506>
- Shi Z.L., Liu F.M. and Yao S.H. (2011) Adsorptive removal of phosphate from aqueous solutions using activated carbon loaded with Fe(III) oxide. *New Carbon Materials* 26(4): 299–306. Available at: [https://doi.org/10.1016/S1872-5805\(11\)60083-8](https://doi.org/10.1016/S1872-5805(11)60083-8)
- Socrates G. (2004) *Infrared and Raman Characteristic Group Frequencies: Tables and Charts*. 3rd edn. Chichester: John Wiley & Sons. ISBN: 978-0470093078
- Srivastava V.C., Swamy M.M., Mall I.D., Prasad B. and Mishra I.M. (2006) Adsorptive removal of phenol by bagasse fly ash and activated carbon: equilibrium, kinetics and thermodynamics. *Colloids and Surfaces A: Physicochemical and Engineering Aspects* 272(1–2): 89–104. Available at: <https://doi.org/10.1016/j.colsurfa.2005.07.016>
- Tawalbeh M., Allawzi M.A. and Kandah M.I. (2005) Production of activated carbon from jojoba seed residue by chemical activation residue using a static bed reactor. *Journal of Applied Sciences* 5(3): 482–487. Available at: <https://doi.org/10.3923/jas.2005.482.487>
- Xie B., Qin J., Wang S., Li X., Sun H. and Chen W. (2020) Adsorption of phenol on commercial activated carbons: modelling and interpretation. *International Journal of Environmental Research and Public Health* 17(3): 789. Available at: <https://doi.org/10.3390/ijerph17030789>
- Yan G., Cai B., Chen C., Wang Q. and Guo S. (2015) Biodegradability evaluation of pollutants in acrylonitrile wastewaters based on particle size distribution. *Desalination and Water Treatment* 53(10): 2792–2798. Available at: <https://doi.org/10.1080/19443994.2014.931530>
- Zhang X., Liu H., Li Y., Li G. and Hu C. (2015) Preparation of activated carbon from pyrolytic residue of rice husk and its application for the adsorption of phenol and iodine. *Asian Journal of Chemistry* 27(4): 1513. Available at: <https://doi.org/10.14233/ajchem.2015.18607>



This article is an Open Access article distributed under the terms and conditions of the Creative Commons Attribution 4.0 (CC BY 4.0) License (<http://creativecommons.org/licenses/by/4.0/>).